

# Detection of Body Position Changes on the Surface ECG

J García\*, M Åström#, P Laguna\*, L Sörnmo#

\*Communications Technologies Group, CPS, University of Zaragoza, Spain

# Department of Applied Electronics, Lund University, Sweden.

## Abstract

*Changes in body position are sometimes mistaken for myocardial ischemia during ECG monitoring in the coronary care unit. Two different methods for detecting body position changes based on spatial and scalar approaches are investigated. These methods have been tested in two databases containing controlled body position changes, and ischemic episodes, respectively. The results show that reliable detection is possible in more than 90 % of the cases.*

## 1. Introduction

Body position changes (BPCs) are sometimes misclassified as ischemic events when monitoring the ECG in the intensive care unit. This observation has been pointed out in a number of recent papers [1], [2]. Previous work are descriptive in nature and present results on how various ECG measurements are affected by changes in body positions; no methodological development concerning the BPC detection problem is presented. The purpose of this paper is to investigate algorithms that reduce ischemic false alarms due to BPCs during ambulatory ischemia monitoring. Two methods which deal with the issue of detecting BPCs are presented: one technique utilizes a spatial approach by estimating rotation angles of the electrical axis, while the other uses scalar-lead signal representation based on the Karhunen-Loève transform (KLT).

## 2. Methods

### 2.1. Spatial approach using rotation angles

The spatial approach assumes that a BPC changes the direction of the electrical axis of the heart. The axis change can be estimated by relating a vectorcardiographic (VCG) loop of the QRS complex (matrix  $\mathbf{Z}$ ) to a reference loop,  $\tilde{\mathbf{Z}}_R$ . The relation is based on certain geometrical transformations i.e., scaling (scalar  $\alpha$ ) and rotation (matrix  $\mathbf{Q}$ ) as well as assuming the presence of additive white Gaussian

noise,  $\mathbf{V}$ . A refined time synchronization is introduced by the shift matrix  $\mathbf{J}_\tau$ . The model relation between  $\mathbf{Z}$  and  $\tilde{\mathbf{Z}}_R$  is expressed as [3],

$$\mathbf{Z} = \alpha \mathbf{Q} \tilde{\mathbf{Z}}_R \mathbf{J}_\tau + \mathbf{V} \quad (1)$$

In ischemia monitoring, it is preferable to select the early part of the QRS complex for loop alignment because the later parts are affected by ischemia. In order to handle large differences in amplitude of the early part, a normalized distance criterion for loop alignment was introduced [4],

$$\epsilon_{min}^2 = \min_{\alpha, \mathbf{Q}, \tau} \frac{\|\mathbf{Z} - \alpha \mathbf{Q} \tilde{\mathbf{Z}}_R \mathbf{J}_\tau\|_F^2}{\|\alpha \mathbf{Q} \tilde{\mathbf{Z}}_R \mathbf{J}_\tau\|_F^2} \quad (2)$$

From (2) it is possible to derive least squares estimates of the alignment parameters  $\hat{\alpha}$  and  $\hat{\mathbf{Q}}$ . The three element (one for each dimension) rotation angle estimate,  $\hat{\varphi}$  is in turn defined by  $\hat{\mathbf{Q}}$ . In order to denote the estimates from different VCG loops, corresponding to different beats, a time notation identifying angle estimate at  $t_i$  is included with the angle estimates,  $\hat{\varphi}(t_i)$ .

In order to improve detector performance, poor angle estimates were rejected based on two different criteria. The first criterion is related to the signal-to-noise ratio (SNR) of the VCG loop, rejecting beats with a low SNR compared to an exponentially weighted average. The second criterion is based on the deviation of the present angle estimate relative to the median absolute deviation of surrounding angle estimates, a too large deviation resulting in rejection. By introducing a delay in the system and also choosing proper parameter settings, changes in angle estimates due to BPCs are not rejected. The method briefly described here is based on the X84 rejection method [5]. Following rejection, resampling of  $\hat{\varphi}(t_i)$  results in the evenly sampled time series  $\hat{\varphi}(k)$ , cf. Fig 1. Matched filters are commonly used for detection of a known signal waveform in noise. Considering BPC detection where the hypothesis is that a BPC is reflected by a step change in the rotation angles of the electrical axis, thus suggesting that

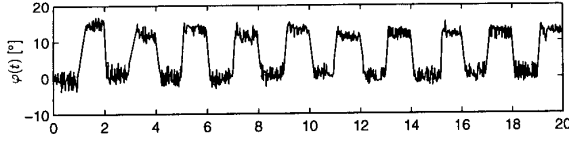


Figure 1: Example of angle estimates during BPCs.

the matched filter therefore should be a step function i.e.,  $h(k) = [-1 \dots -1 \ 1 \dots 1]$ . However, due to rejection of angle estimates, the transition from one position to another may not be instantaneous and is therefore here modeled as a linear slope in the interval  $[1 \ \theta_k]$  where  $\theta_k$  is the number of samples previously removed. The matched filter can thus be expressed as

$$h(n; \theta_k) = \begin{cases} -1, & n = -N + 1, \dots, 0 \\ -1 + \frac{2n}{\theta_k}, & n = 1, \dots, \theta_k \\ 1, & n = \theta_k + 1, \dots, \theta_k + N \end{cases} \quad (3)$$

The output of the matched filter is squared resulting in a signal  $\mu(k)$ ,

$$\mu(k) = |\hat{\varphi}_X(k) * h(n, \theta_k)|^2 \quad (4)$$

which is suitable for making a decision on whether a BPC has occurred or not. A BPC is identified if the energy,  $g_A(l)$ ,

$$g_A(l) = \frac{1}{k_l^e - k_l^b} \sum_{k=k_l^b}^{k_l^e} \mu(k) \quad (5)$$

of a sequence of samples,  $[k_l^b \ k_l^e]$ , exceeds a certain threshold,  $\Gamma$ . The BPC is then identified as the centre of gravity of  $\mu(k)$  in the interval. The parameters defining the summation limits,  $k_l^b$  and  $k_l^e$ , are given from the following conditions,

$$\begin{bmatrix} \mu(k_l^e) & \mu(k_{l+1}^b) \end{bmatrix} \geq \mu_s \quad \text{or} \quad \begin{bmatrix} \mu(k_l^b) & \mu(k_l^e) \end{bmatrix} \geq \mu_l \quad \text{or} \quad k_l^e + K_r < k_{l+1}^b \quad (6)$$

in which  $\mu_l$  and  $\mu_s$  are limits of large and small amplitude levels, respectively. The reason for this is to separate potential BPCs ( $\mu(k) > \mu_l$ ) from certain nonBPCs ( $\mu(k) < \mu_s$ ).  $K_r$  is a refractory period during which no sample should exceed  $\mu_l$  introduced in order to separate two BPCs from each other.

## 2.2. Scalar approach based on KLT

The KLT technique applied to the different waves of the ECG provides a useful tool to characterize their mor-

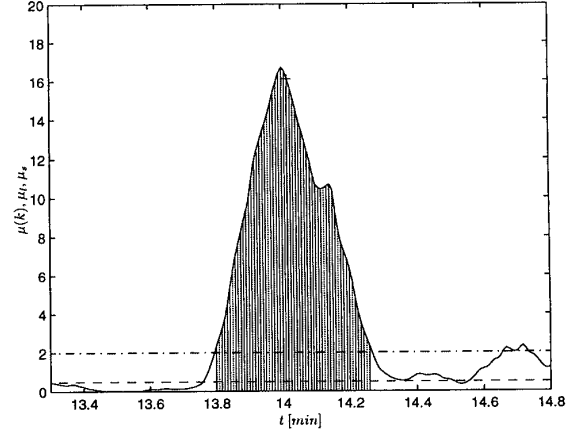


Figure 2: Illustration of the detection algorithm described in Sec. 2.1.. In the figure,  $\mu_l = 2$  (dash-dotted) and  $\mu_s = 0.5$  (dashed). The striped area,  $g_A(l)$  is limited by  $k_l^b$  and  $k_l^e$ . The parameter  $K_r = 5$  s, resulting in that the complex at 14.7 s is too distant to be part of the large complex at 14 s. The small complex is not sufficiently large to qualify as a BPC on its own.

phologic changes [6, 7]. The scalar detector structure calculates a combined distance function,  $\mathcal{F}(t_i)$ , for the QRS and ST-T complexes according to the expression

$$\mathcal{F}(t_i) = \lambda_{QRS} \cdot f_{QRS}(t_i) + \lambda_{STT} \cdot f_{STT}(t_i) \quad (7)$$

where  $\lambda_{QRS}$ ,  $\lambda_{STT}$  represent the weights for the functions (experimentally selected to 0.8 and 0.2, respectively, since ischemia affects mainly ST-T complex whereas a BPC affects more the QRS complex), and  $f_{QRS}$ ,  $f_{STT}$  are the distance functions for each complex defined as

$$f(t_i) = \sum_{j=1}^3 \left( \sum_{m=0}^3 (\alpha_m^j(t_i) - \alpha_m^j(ref))^2 \right)^{\frac{1}{2}} \quad (8)$$

with  $\alpha_m^j(t_i)$  being the  $m$ :th order KLT coefficient at instant  $t_i$  for the  $j$ :th lead, and  $\alpha_m^j(ref)$  the mean reference value estimated from the first 20 beats of the recording. The  $\mathcal{F}(t_i)$  function will in a combined way reflect changes in QRS and ST-T complexes.

Again,  $\mathcal{F}(t_i)$  is evenly resampled and a matched filter with a step-shaped impulse response is used, followed by a detector based on the use of a constant false alarm rate (CFAR) strategy. CFAR detectors are used in radar systems [8] and are based on the design presented in Fig. 3. In a CFAR detector, each sample,  $x(k)$ , is compared (by using a comparator,  $C: x(k) > x(k+n)$ ,  $n = [-\frac{M}{2} \dots -1 \ 1 \dots \frac{M}{2}]$ ) to its  $M$  neighbors

and the number of cases in which this comparison is positive,  $r$ , is determined. Then this rank number,  $r$ , has to exceed a threshold,  $\eta$ , to consider that a detection occur in that sample. The threshold thereby depends on the values of the surrounding samples. To avoid detecting very small

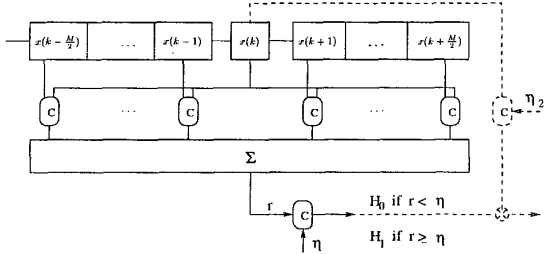


Figure 3: Basic design of a constant false alarm rate (CFAR) detector, and modification added to avoid very small peaks detection (dashed lines).

peaks (low amplitude samples in the matched filter output with lower values in the neighborhood) the classical design was modified adding a second threshold,  $\eta_2$ , needed for a sample to represent a detection ( $x(k) \geq \eta_2$ ); (see modification in Fig. 3, in dashed lines).

An example of the performance of the KLT-CFAR detector is shown in Fig. 4 with annotated BPCs occurring each minute. In the top panel, the estimated  $\mathcal{F}(t)$  function is represented together with the BPC detections (+), and the annotated instants of BPCs ( $\Delta$ ). In the bottom panel the corresponding rectified matched filter output is represented.

### 3. Study population

First, a database (BPC-DB) which contains ECG recordings with a predefined protocol of BPCs was considered. Each of the 20 recording lasts for 20 minutes and presents the BPC pattern of *supine—right side—supine—left side*, one change taking place every minute. Standard 12-lead ECG was recorded using low-noise ECG amplifiers (Siemens—Elema AB, Solna, Sweden). The signal was digitized at a sampling rate of 1 KHz with an amplitude resolution of  $0.6 \mu V$ . A brief survey revealed that BPC-induced changes affected both depolarization (QRS complex) and repolarization (ST-T complex) intervals. The influence of BPCs on the repolarization phase was analyzed looking at changes induced in STJ60 level (up to  $180 \mu V$ ) and T wave amplitude (up to  $600 \mu V$ ), that could eventually yield false positives in ischemia detectors. In Fig. 5 the differences in the ECG for the three recording positions in one subject are shown.

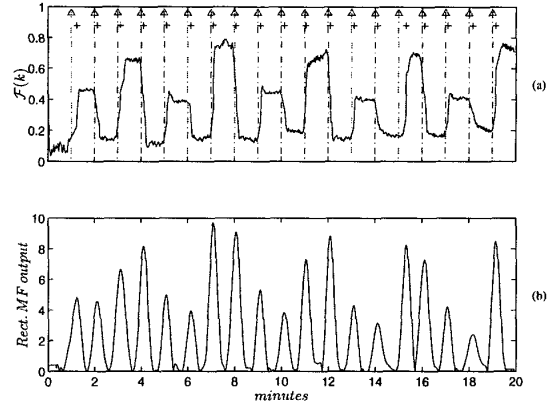


Figure 4: BPC detection example: (a)  $\mathcal{F}(k)$  function together with BPCs occurrences ( $\Delta$ ) and detections (+); (b) rectified matched filter output of the  $\mathcal{F}(k)$  function.

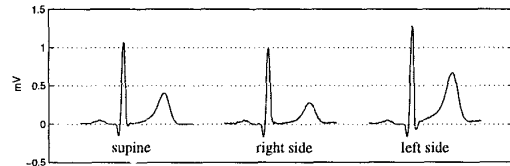


Figure 5: Beat waveforms for the three positions of recording in the same subject.

Second, a database (STAFF III-DB) containing ECG recordings obtained during prolonged percutaneous transluminal coronary angioplasty (PTCA) as well as a corresponding control recording, recorded prior to the intervention, was evaluated. The STAFF III-DB was previously used to evaluate the sensitivity of different indexes regarding ischemia [9] and in this work will be considered with the purpose to serve as a reference to measure the false detections of ischemic events as BPCs in the BPC detectors.

### 4. Results

The evaluation of the detector performance was done in terms of sensitivity,  $S = \frac{TP}{TP+FN}$ , (where  $TP$  and  $FN$  denotes *true positives* and *false negatives*, respectively) and positive predictivity,  $+P = \frac{TP}{TP+FP}$ , (with  $FP$  denoting *false positives*) in the BPC-DB, and of number of false positives per hour ( $FPh^{-1}$ ) in the STAFF III-DB. The results, obtained after application of the two methods are shown in Tab.1.

Table 1: Performance statistics for the BPC detectors on the BPC-DB and STAFF III-DB. In the STAFF III-DB it is distinguished between control ( $c$ ) and angioplasty ( $a$ ) recordings.

detector	BPC-DB		STAFF III-DB
	$S$	$+P$	$FPh^{-1}(c/a)$
Spatial appr.	90 %	98 %	3.9 / 25.5
Scalar appr.	97 %	97 %	20.0 / 35.1

## 5. Discussion

Matching between annotated BPCs and detections by the system were considered within an acceptance interval of 25 s. The reason for using such a long interval is the presence of noisy beats around the BPC instant (the noisy beats intervals were found to last up to 10 s).

Both detectors showed an acceptable performance on the BPC-DB, but performed worse on the STAFF III-DB. However, in some respect the results of the two methods differ. The scalar approach has a higher  $S$  for the BPC-DB which is compensated by a lower  $FPh^{-1}$  for the spatial approach. No conclusions could be made from these results, regarding which method is the better one, since a higher  $S$  value also implies a higher  $FPh^{-1}$ .

The varying results of the detectors concerning the two databases may be explained by their properties. The BPC database consists of well defined events recorded in an ideal environment, whereas the STAFF III database may not be the best one for representing ischemic episodes commonly found in CCUs, since it is composed of ECGs corresponding to sudden coronary occlusions. Therefore, the real performance of the algorithms could be expected to decrease for  $S$  and  $+P$  and increase for  $FPh^{-1}$ .

A BPC episode usually implied a few noisy beats (due to myomuscular noise) around its location (a noisy beat can be a low SNR beat or a beat with high baseline wandering). It is possible to use the reverse (negative) implication to reject possible false BPC detections in the following way: no noisy beats found imply no BPC. Preliminary results show that this extension is promising but further research is needed on this direction.

## 6. Conclusions

This paper has shown that reliable detection of BPCs is possible with methods based on both spatial and scalar approaches. Further research is needed to study the detector performance in a wider variety of both BPC recordings as well as ischemic recordings in order to determine which method can work more efficiently for ambulatory

purposes.

## Acknowledgements

This work was supported by NUTEK, grant no. 89-03381P (Sweden) and by projects TIC97-0945-C02-02 from CICYT, PIT40/98 from CONSI+D and 2FD97-1197-C02-01 from FEDER (Spain). This study is part of the STAFF Studies.

## References

- [1] M.G. Adams and B.J. Drew, "Body position effects on the electrocardiogram: implications for ischemia monitoring", *J. of Electrocardiology*, vol. 30, no. 4, pp. 285–291, 1997.
- [2] T. Jernberg, B. Lindahl, M. Högborg, and L. Wallentin, "Effects on QRS-waveforms and ST-T-segment by changes in body position during continuous 12-lead ECG: A preliminary report", in *Computers in Cardiology*. IEEE Comp. Soc., 1997, pp. 461–464.
- [3] L. Sörnmo, "Vectorcardiographic loop alignment and morphologic beat-to-beat variability", *IEEE Trans. Biomed. Eng.*, vol. 45, no. 12, pp. 1401–1413, December 1998.
- [4] M. Åström, L. Sörnmo, J. García, and P. Laguna, "Least squares vcg loop alignment", in *Proc. of Biosignal Interpretation*, 1999, pp. 265–268.
- [5] F. Hampel, E. Ronchetti, P. Rousseeuw, and W. Stahel, *Robust Statistics*, Wiley Series in Probability and Mathematical Statistics. John Wiley & Sons, New York, USA, 1986.
- [6] P. Laguna, G.B. Moody, J. García, A.L. Goldberger, and R.G. Mark, "Analysis of the ST-T complex of the electrocardiogram using the Karhunen-Loève transform: adaptive monitoring and alternans detection", *Med. Biol. Eng. Comput.*, vol. 37, pp. 175–189, 1999.
- [7] J. García, G. Wagner, L. Sörnmo, S. Olmos, P. Lander, and P. Laguna, "Temporal evolution of ECG-based indexes in patients with myocardial ischemia induced by prolonged balloon occlusion", in *Computers in Cardiology*. IEEE Computer Society Press, 1998, pp. 293–296.
- [8] N. Levanon, *Radar principles*, John Wiley & Sons, New York, 1988.
- [9] J. García, P. Lander, L. Sörnmo, S. Olmos, G. Wagner, and P. Laguna, "Comparative study of local and Karhunen-Loève based ST-T indexes in recordings from human subjects with induced myocardial ischemia", *Computers and Biomedical Research*, vol. 31, pp. 271–292, August 1998.

### Address for correspondence:

J. García  
 Dep. Ing. Electrónica y Comunicaciones  
 Maria de Luna 3. 50015-Zaragoza (SPAIN)  
 E-mail: jogarmo@posta.unizar.es